

# Study of the Effect of Nitrogen on Corrosion, Wear resistance and Adhesion Properties of DLC Films Deposited on AISI 321H

L. S. Almeida<sup>a,\*</sup> , M. S. Pereira<sup>b</sup>, C. A. Antônio Junior<sup>a</sup>, F. C. Silva<sup>c,d,e</sup>, O.M. Prada Ramirez<sup>c</sup> ,  
C. G. Schön<sup>c</sup>, H.G. de Melo<sup>c</sup> , M. D. Manfrinato<sup>a,b</sup> , L. S. Rossino<sup>a,b</sup>

<sup>a</sup>Universidade Federal de São Carlos – UFSCar, Rodovia João Leme dos Santos, Km 110, Bairro do Itinga, 13069-700, Sorocaba, SP, Brasil.

<sup>b</sup>Faculdade de Tecnologia de Sorocaba – FATEC SO, Av. Engenheiro Carlos Reinaldo Mendes, 2015, Além Ponte, 13013-280, Sorocaba, SP, Brasil.

<sup>c</sup>Universidade de São Paulo, Escola Politécnica, Departamento de Engenharia Metalúrgica e de Materiais, Avenida Prof. Mello Moraes, 2463, 05508-030, São Paulo, SP, Brasil.

<sup>d</sup>Faculdade de Tecnologia do Estado de São Paulo – FATEC Cotia, Centro Estadual de Educação Tecnológica Paula Souza, Rua Nelson Raineri, 700, 06702-155, Cotia, SP, Brasil.

<sup>e</sup>Faculdade de Tecnologia do Estado de São Paulo – FATEC São Paulo, Centro Estadual de Educação Tecnológica Paula Souza, Avenida Tiradentes, 615, 01124-060, São Paulo, SP, Brasil.

Received: March 18, 2022; Revised: August 01, 2022; Accepted: September 11, 2022

The deposition of DLC films on 321H stainless steel aims at attributing properties such as high wear resistance and low friction coefficient to the substrate material. Nitrogen added to DLC can improve the film adhesion to metal substrates, but the investigation of its effect on corrosion resistance, an important property for stainless steels, is lacking. The DLC film was deposited by plasma-enhanced chemical vapor deposition (PECVD) using a pulsed-DC power supply with a gas mixture of Ar and CH<sub>4</sub>, and to the DLC(N) film deposition was used CH<sub>4</sub> and N<sub>2</sub> varying the percentage of nitrogen from 10 to 50% in the treatment. DLC films improved both the wear and corrosion resistance of 321H stainless steel. The results show that the 10, 20 and 30% of N<sub>2</sub> supply during the deposition increased the adhesion of the film on the substrate, enhancing the wear resistance of the treated material. The addition of 40 and 50% of N<sub>2</sub> during the deposition, however, impaired the corrosion resistance compared with the substrate. An improvement of adhesion, wear and corrosion resistance were observed for 30% N<sub>2</sub> condition. Thus, the incorporation of suitable concentration of nitrogen modifies the features of the DLC film, obtaining a good combination of high wear resistance and corrosion protection due to a combination of structure, high thickness, and high adhesion of the film to 321H stainless steel.

**Keywords:** *micro-abrasive wear, DLC, corrosion potential, nitrogen.*

## 1. Introduction

AISI 321H austenitic stainless steel was developed with the main intention to avoid sensitization by the addition of titanium, which stabilizes the metal and inhibits the formation of grain boundary chromium carbides<sup>1</sup>. This kind of stainless steel, after stabilization heat treatment, can be used in equipment in the petrochemical industry operating in the temperature range from 450° C to 800° C<sup>2</sup>. However, titanium nitrides inclusions observed in this material can act as a cathode and influence the corrosion behavior of the material<sup>3</sup>.

Carbon is one of the most important alloying elements in steels, and it is found in several allotropic variants, such as diamond and graphite, for example, showing a wide range of properties<sup>4</sup>. DLC films (diamond like-carbon films) have caught the attention in the literature due to their unique properties, such as excellent wear resistance, biocompatibility, chemical inertia, characteristics as a solid

lubricant, and proper corrosion resistance<sup>5-8</sup>. These properties are influenced by the combination of the sp<sup>2</sup> and sp<sup>3</sup> C-C bond, whose sp<sup>3</sup> hybridization is characteristic of the diamond providing the mechanical properties of the film, while the sp<sup>2</sup> hybridization is found in graphite, providing the lubricant features of the film<sup>5,9</sup>. Hence, DLC films deposited on 321H stainless steels are expected to improve surface properties, such as high hardness, high wear resistance, and low friction coefficient to this material<sup>5-8</sup>. It is possible, however, that the inherent defects of this film could impair the corrosion resistance of the treated material<sup>10,11</sup>.

Several works report the effect of the DLC doping on their property modification using different elements<sup>12-18</sup>, such as nitrogen that added to DLC films can considerably improve its adhesion to metallic substrates<sup>19</sup>, with a great influence on the effectiveness of corrosion protection and wear resistance of the treated material<sup>20,21</sup>. Almeida et al.<sup>21</sup> observed that the introduction of intermediate amounts of N<sub>2</sub> (30%) on the DLC film by PECVD reduces the fraction of sp<sup>3</sup> bonds

\*e-mail: [solano.larissa@gmail.com](mailto:solano.larissa@gmail.com)

keeping the mechanical characteristics of the DLC film, and improving the wear and adhesion of the film to the metallic substrate. Sharifahmadian et al.<sup>12</sup> have observed that nitrogen-doped DLC films impair the corrosion resistance of the material, however, only one treatment parameter was investigated<sup>12</sup>. Studying the corrosion behavior of the ta-C:N thin film doped with nitrogen deposited on p-Si(111) substrate, Khun et al.<sup>22</sup> determined that the polarization results showed that the corrosion resistance of the films dropped with increased nitrogen flow rate due to formation of more sp<sup>2</sup> bonds<sup>22</sup>, whose result was opposite to that obtained by Han et al.<sup>23</sup>.

The effect of adding nitrogen concerning the corrosion resistance of DLC films deposited on stainless steel is still lacking<sup>12</sup>. The objective of this work is to investigate the effect of nitrogen incorporation on the adhesion, corrosion, and wear resistance of the DLC films deposited on 321H stainless steels.

## 2. Materials and Methods

### 2.1. Deposition of the films

The stainless steel 321H substrate was subjected to surface preparation processes, such as cutting, sanding, polishing, and cleaning with ultrasound water with soap and alcohol to remove any residue from the preparation.

The deposition of the DLC and DLC(N) films was carried out by plasma-enhanced chemical vapor deposition (PECVD), with a system already described by Cruz et al.<sup>24</sup>, at the Laboratory of Surface Technology and Engineering (LabTES) of the Technological College of Sorocaba (FATEC-SO).

The deposition of the DLC and DLC(N) films was carried out in three stages, starting with a superficial cleaning by plasma ablation process using 80% Ar and 20% H<sub>2</sub> at a working pressure of 2.00 torr for 30 min, parameters that provide efficient cleaning of the metallic surface<sup>21</sup>. Thereafter, the deposition of a silicon-based layer was carried out, using hexamethyldisiloxane (HMDSO) as a precursor, with 70% HMDSO and 30% Ar at a total gas pressure of 0.06 torr for 15 min. Then, the deposition of the DLC or DLC(N) films was carried out with the parameters based on the study carried out by Almeida et al.<sup>19</sup>. The substitution of argon for nitrogen in the gas mixture for the DLC(N) films followed the studies carried out by Franceschini and Freire<sup>25</sup> and Franceschini, Freire and Silva<sup>16</sup>. The parameters are described in Table 1.

### 2.2. Characterization

Samples without and with DLC and DLC(N) films were characterized by micro-abrasive wear test, scanning electron microscopy (SEM) analysis, Raman spectroscopy, adhesion test, and the electrochemical techniques of potentiodynamic polarization and electrochemical impedance spectroscopy.

The wear behavior of the treated and untreated samples was determined by a micro-abrasive wear test by fixed ball<sup>26,27</sup> using a steel sphere (AISI 52100) with radius (*r*) of 12.7 mm under dry condition (no abrasive and lubrication) and conducted at room temperature. A normal load of 8 N, rotation of 40 Hz during 600 s were used on all tests, which were performed in duplicate to ensure reproducibility. The wear volume (*V*) was defined by Equation 1, as described by Rutherford and Hutchings<sup>28</sup>. After the test, the wear surface was analyzed by optical microscopy (OM) using a Leica model DMi8 C.

$$V = \frac{\pi b^4}{64r} \quad (1)$$

where “*b*” denotes the diameter of the wear crater and “*r*” the radius of the standard ball used in the test.

The corroded region and microstructural analysis of the produced films was carried out by scanning electron microscopy (SEM) using a Hitachi TM 3000 equipment with a voltage of 15 kV and back-scattered electron (BSE) detector. The semi-quantitative chemical composition of the DLC and DLC(N) film was determined using energy dispersive spectroscopy (EDS). The fraction analysis of the film defects was carried out by SEM with magnification of 500x using the software ImageJ<sup>®</sup>, considering the color difference between the areas with defects (white) and DLC film (black).

Raman spectroscopy is a technique widely used to characterize DLC coatings and other carbon-based materials<sup>23,29</sup>. This analysis allows evaluating chemical structure of the films, identify *D* and *G* band peak positions, determine *I<sub>D</sub>*/*I<sub>G</sub>* ratio, and the width of half of band *G* (FWHM(*G*)) a useful tool to correlate mechanical, adhesion, tribological, and corrosion behavior with the DLC coatings deposition conditions<sup>23,30,31</sup>. Therefore, to characterize the DLC and DLC(N) coatings deposited by PECVD, a Renishaw – in Via Raman Microscope was used, with an argon laser with 5 μm of diameter spot, the wavelength of 514 nm and power of 5%. Equation 2 was used to estimate the hydrogen content in the DLC film<sup>32</sup>.

**Table 1.** Parameters of the DLC and DLC(N) films deposition.

Treatments	DLC and DLC(N) films				
	Gases Percentage (%)	Total flow (sccm)	Voltage (V)	Time (h)	Temperature (°C)
DLC	90 CH <sub>4</sub> + 10 Ar	40	500	2	± 200
DLC(N) 10% N <sub>2</sub>	90 CH <sub>4</sub> + 10 N <sub>2</sub>				
DLC(N) 20% N <sub>2</sub>	80 CH <sub>4</sub> + 20 N <sub>2</sub>				
DLC(N) 30% N <sub>2</sub>	70 CH <sub>4</sub> + 30 N <sub>2</sub>				
DLC(N) 40% N <sub>2</sub>	60 CH <sub>4</sub> + 40 N <sub>2</sub>				
DLC(N) 50% N <sub>2</sub>	50 CH <sub>4</sub> + 50 N <sub>2</sub>				

$$H[\%] = 21.7 + 16.6 \log \frac{m}{I_{(G)}} [\mu m] \quad (2)$$

where  $I(G)$  is the intensity of G band and  $m$  is the inclination of spectra between 1000 and 1800  $\text{cm}^{-1}$ .

Rockwell-C adhesion tests were performed to investigate the adhesion features of DLC and DLC(N) coatings on the metal surface<sup>33,34</sup>. To assess layer damage on the boundary of indentation produced on the coating surface, SEM Hitachi TM 3000 equipment was used to analyze the surface. ImageJ® software was used to calculate the delaminated region compared to the non-delaminated region, as detailed in<sup>33</sup>.

Electrochemical tests were carried out in the treated and untreated material using a Potentiostat/Galvanostat/ZRA Gamry Instruments Model Reference 600+ at room temperature (25 °C) in 0.6 mol/L NaCl solution. All tests were carried out with a three-electrode cell, using the uncoated (AISI 321), DLC, and DLC(N) coated samples as working electrodes (exposed area of 0.85  $\text{cm}^2$ ). A platinum wire and Ag/AgCl were used as counter and reference electrodes, respectively. The potentiodynamic polarization curves were obtained after 30 min of open circuit potential (OCP) stabilization, and the tests were performed from -0.25 V vs OCP to  $1 \times 10^{-4}$  A. $\text{cm}^{-2}$  at a scan rate of 1 mV/s in the anodic direction. Electrochemical impedance spectroscopy (EIS) measurements were carried out after 3600 s stabilization of the open circuit potential (OCP) applying an alternate current (ac) signal of 15 mV (rms) in a frequency range from  $10^5$  Hz to  $10^{-2}$  Hz with an acquisition rate of seven points per decade.

### 3. Results and Discussion

#### 3.1. Morphological and mechanical characterization

The analysis of the Raman spectrum of the DLC film (Figure 1a) shows the D band around 1350  $\text{cm}^{-1}$ , which is related to the defects of the  $\text{sp}^2$  carbon network, and the G band around 1540  $\text{cm}^{-1}$ , related to the expansion of the  $\text{sp}^2$  carbon atom sites<sup>35</sup>. According to Equation 2, the estimated atomic fraction of hydrogen in the film is 34.9%.

The result evidences the formation of the hard hydrogenated amorphous carbon a-C:H film on the 321H stainless steel substrate, as classified by Robertson<sup>9</sup>.

In Figure 1a, it is also possible to notice a shift in the position and intensity of the D and G bands due to the incorporation of nitrogen into the a-C:H film<sup>19</sup>. Figure 1b shows the  $I_D/I_G$  ratios for all films obtained from 0 to 50%  $\text{N}_2$ . The increase in the  $\text{N}_2$  percentage added to the treatment increased the  $I_D/I_G$  ratio due to enhanced nitrogen incorporation on the film, indicating an increase in the graphitic network ( $\text{sp}^2$ ), once the doping of the DLC films with nitrogen favors the bonding of nitrogen atoms with carbon atoms, generating C-C  $\text{sp}^2$  bonds<sup>36</sup>. Several works attributed an improvement of anti-corrosion resistance and impedance for DLC coatings by the highest amount of C-C  $\text{sp}^3$  bonds, which is directly related to a decrease of  $I_D/I_G$  ratio, presenting a diamond-like behavior. On the other hand, to improve surface adhesion, wear resistance and decrease friction coefficient, graphite-like behavior depends on the presence of C-C  $\text{sp}^2$  bonds. Hence, it is possible to combine the properties and features of the produced DLC films by controlling the deposition parameters or by adding chemical elements, allowing changes in the  $\text{sp}^2/\text{sp}^3$  ratio, opening a variety of possibilities and applications from DLC coatings<sup>23,31</sup>.

Figure 1c allows to observe the width at half-height of the G band (FWHM(G)) for DLC and DLC(N) films. The structural disorder of the DLC film can be determined by the FWHM(G), which occurs by the distortion of the angle and the length of the film bonds. The FWHM(G) parameter increases with increasing structural disorder<sup>9,32</sup>. Thus, we can observe that the addition of 10% of  $\text{N}_2$  in the treatment generates an increase in the structural disorder, which is related to the increase in the C-C  $\text{sp}^3$  bond proportion. However, with the continuous increase of the  $\text{N}_2$  amount in the treatment, a decrease in FWHM(G) is observed, indicating a decrease in the disorder of the film, as well as of the C-C  $\text{sp}^3$  bond proportion, corroborating with the  $I_D/I_G$  ratio analysis, which influences on decreasing mechanical properties of the film<sup>32</sup> and could be an indicative for improvement of corrosion resistance.

In Figure 2a-f) are presented the micrographs of the cross sections of the samples with DLC and DLC(N) films with 0, 10, 20, 30, 40 and 50%  $\text{N}_2$ , respectively. The EDS

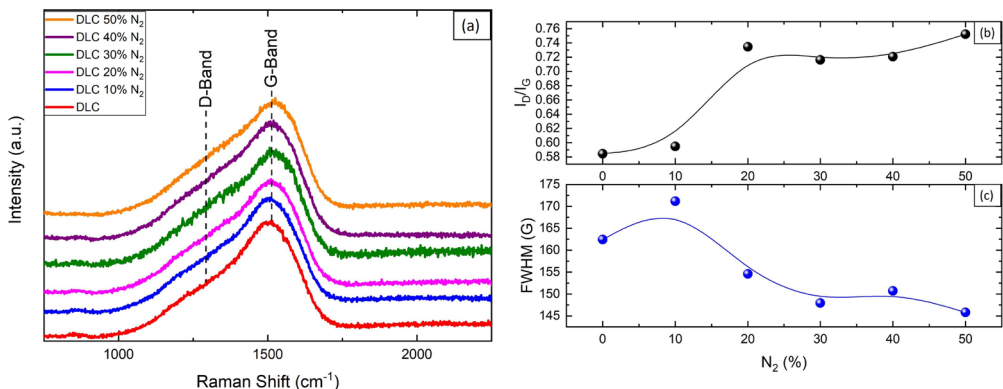


**Figure 1.** (a) Raman spectra of DLC and DLC(N) films (b)  $I_D/I_G$  ratio of the DLC and DLC(N) films, and (c) FWHM(G) analysis of the DLC and DLC(N) film from 0 to 50%  $\text{N}_2$ .

analysis presented in Figure 2g-h prove the film formation, with the high intensity of carbon for the DLC film and the presence of carbon and nitrogen for the DLC(N) films. It is observed that the obtained films are homogeneous.

According to Figure 3a, DLC film presents a thicker layer compared to nitrogenated films, showing that the increased nitrogen supply during deposition influences the thickness of the coatings. Comparing the behavior of the nitrogenated films, DLC(N) 30% N<sub>2</sub> condition presents a thicker layer, and DLC(N) 50% N<sub>2</sub> presents a thinner layer. Besides, deposition conditions with up to 30% N<sub>2</sub> indicate an increased relationship of thickness with the nitrogen supply, with a linear increase in the thickness with the increase in the nitrogen supply from 10 to 20% of N<sub>2</sub>, and the tendency of stability between 20 and 30% of N<sub>2</sub>. However, this growing behavior does not occur for N<sub>2</sub> concentrations higher than 30%, leading to decreased thickness.

This behavior is explained by two factors. The increase of the nitrogen supply in the treatment decreases the number of carbon atoms in the deposition process, leading to thinner layer formation. Also, the high ionization potential of methane (CH<sub>4</sub>) can induce the decreased deposition rate of the film<sup>9</sup>. Comparing the gases proportions (CH<sub>4</sub> and N<sub>2</sub>) for

the different treatment conditions presented in Table 1, these combined factors tend to influence on decrease thickness from 30% N<sub>2</sub>, whose specific condition exhibit a balance on gases concentration from this point, increasing the amount of nitrogen atoms and hindering the film growth. Also, as discussed by Almeida et al.<sup>19</sup>, the increase in nitrogen supply during deposition causes an increase in the nitrogen incorporation in the film.

The defects percentage in the DLC and DLC(N) films did not show a great difference between them, with the maximum value obtained for 50% of N<sub>2</sub> supply in the treatment of 1.5%, followed by 1.28% for 20% of N<sub>2</sub> and the minimum value was observed for the film produced with 10% of N<sub>2</sub>, with 0.2% of defects. Furthermore, analyzing Figure 3b and c, we can observe a correlation with the defects percentage and delamination percentage of the DLC and DLC(N) films up to 30% of N<sub>2</sub>, without correlation with the thickness of the films. The presence of nitrogen in the treatment did not show a pronounced relationship with the defects formed in the film.

It is observed that all DLC and DLC(N) films showed acceptable failures, with the classifications HF1, HF2 and HF3 in the evaluation of the adhesion of the film to the metallic substrate<sup>33</sup>, as can be seen in Table 2. As already

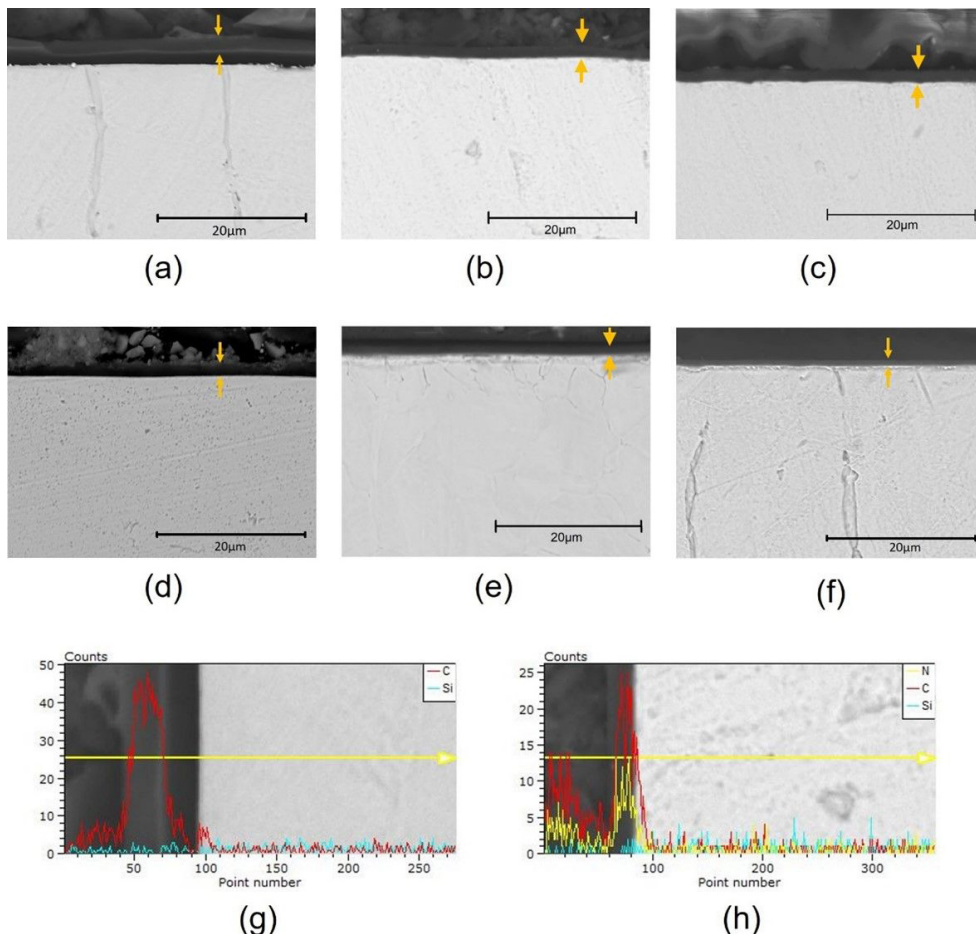


**Figure 2.** Cross-sectional micrograph of films (a) DLC, (b) DLC(N) 10% N<sub>2</sub>, (c) DLC(N) 20% N<sub>2</sub>, (d) DLC(N) 30% N<sub>2</sub>, (e) DLC(N) 40% N<sub>2</sub>, (f) DLC(N) 50% N<sub>2</sub> (g) EDS by SEM of the DLC film and (h) EDS by SEM of the DLC(N) 10% N<sub>2</sub>.

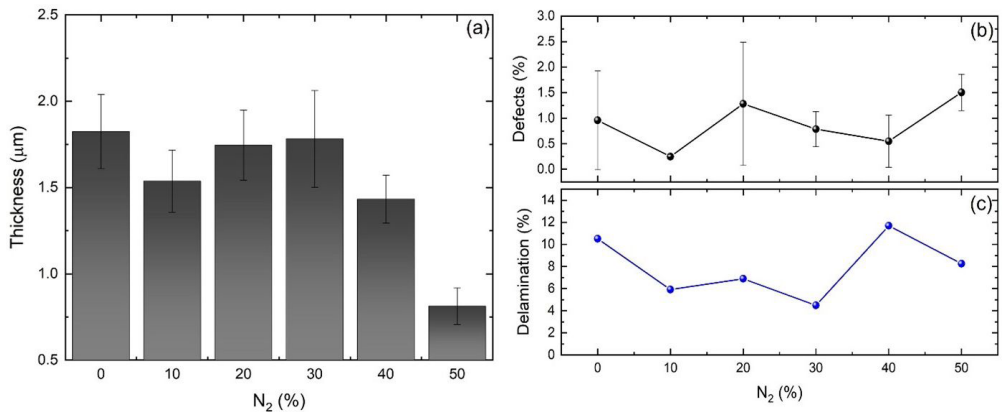


**Figure 3.** Results analysis of the DLC and DLC(N) films (a) thickness, (b) defects, and (c) delamination fraction.

reported in other studies<sup>19,37</sup>, the incorporation of nitrogen favors the adhesion of DLC films, as nitrogen reduces the residual stresses of the film. However, the data in Figure 3 shows that the incorporation of nitrogen improves the adhesion of the DLC film until the percentage of 30% N<sub>2</sub>, which presented the lowest percentage of delamination compared to the other films. Also, it could not be observed a relationship between the thicknesses of the layers and the adhesion properties of the formed films.

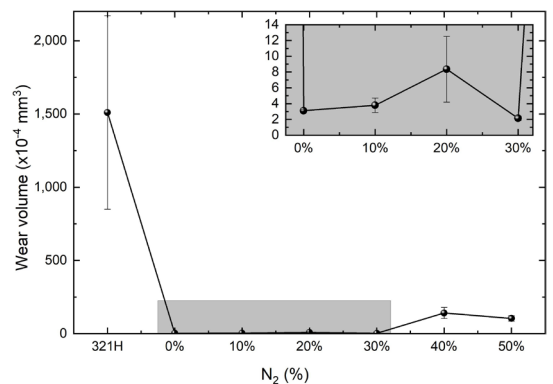
It is already known that adhesion to the substrate has a direct influence on the wear resistance of DLC films<sup>11,19,21</sup>. Figure 4 shows the wear volume of DLC and DLC(N) films from 0 to 50% N<sub>2</sub>. It is observed that all deposited films showed higher wear resistance than the 321H stainless steel substrate without film, explained by the low friction coefficient and high hardness attributed to these films<sup>19</sup>. However, the film with 30% N<sub>2</sub> had the lowest wear volume compared to all films. This result corroborates with that observed by Almeida et al.<sup>19</sup>, ascribed to the higher proportion of C–C sp<sup>3</sup> bonds, lower proportion of C–N sp<sup>3</sup> bonds obtained in the DLC film with 30% N<sub>2</sub>, resulting in better adhesion behavior and thicker layer formation. The worst wear resistance was observed for the DLC(N) 40% N<sub>2</sub> and DLC(N) 50% N<sub>2</sub>, whose presented thinner film formation associated with larger delaminated area.

Figure 5 shows the craters produced in the wear tests. The predominant wear mechanism was rolling, that occurs when the abrasive particles or the particles formed during the test stay free to roll between the surfaces in contact<sup>38</sup>. This three-body process is dominant at low loads and/or high slurry concentration, at which the particles produce high deformation and indentation without preferential direction<sup>39</sup>.

### 3.2. Electrochemical tests

#### 3.2.1. Potentiodynamic polarization experiments

Figure 6 shows the potentiodynamic polarization curves for the AISI 321H steel without and with film deposition. The uncoated sample and most of the coated samples presented a quasi-stationary current density value with increasing potential at the anodic branch characterizing a passive behavior. This was not verified for the samples DLC(N) 40% N<sub>2</sub> and DLC(N) 50% N<sub>2</sub>, which exhibit an



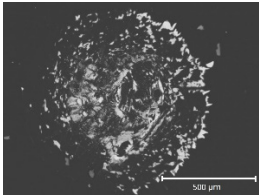
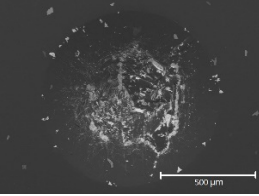
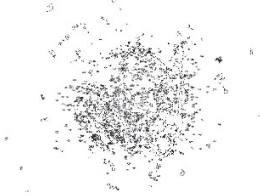
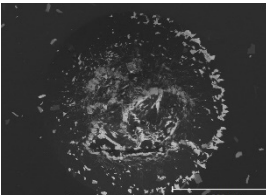
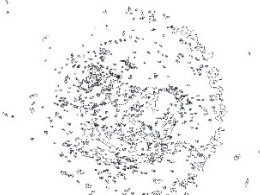
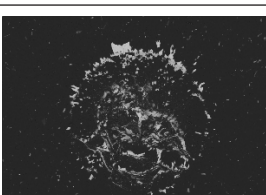
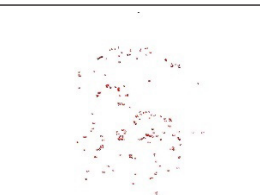
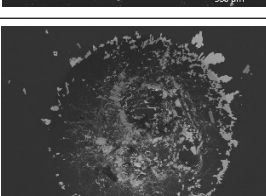
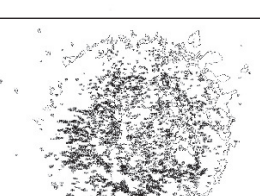
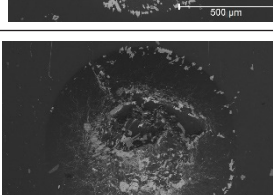
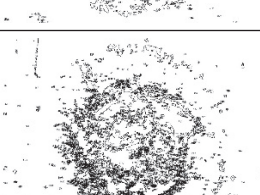
**Figure 4.** Wear volume of the studied material with and without treatment.

active anodic behavior, pointing to increased susceptibility to localized corrosion compared to the base material and to the other coated samples.

In Table 3 are summarized the electrochemical parameters obtained from the polarization curves displayed in Figure 6. The DLC presented the highest  $E_{corr}$  11.50 (mV vs Ag/AgCl) compared to the other samples. DLC(N) 10% N<sub>2</sub>, DLC(N) 20% N<sub>2</sub> and DLC(N) 30% N<sub>2</sub> showed very similar  $E_{corr}$ : -11.0, -11.6 and -17.5 mV vs. Ag/AgCl, respectively, which, nevertheless, were still slightly nobler than the uncoated AISI 321H: -37.60 mV vs Ag/AgCl. On the other hand, the DLC(N) 40% N<sub>2</sub> and DLC(N) 50% N<sub>2</sub> samples, besides showing active behavior, presented the lowest  $E_{corr}$ : -90.8 (mV vs Ag/AgCl) and -262.5 (mV vs Ag/AgCl), respectively. Interestingly, all the coated samples exhibiting passive behavior showed  $E_{corr}$  higher than the uncoated AISI 321H, indicating that the undetective coatings lead to an ennoblement of the substrate.

Table 3 also displays the values of corrosion current density ( $i_{corr}$ ) for all the samples. For those exhibiting passive behavior  $i_{corr}$  was determined by extrapolating the passive current density to the corrosion potential, whereas extrapolation of the anodic branch was adopted as the methodology for the samples exhibiting active response. As the passive current density slightly increases with potential, the passive current densities ( $i_{pass}$ ) were not determined; however, for each sample, it can be assumed that it is similar to its respective  $i_{corr}$ . For the

**Table 2.** Analysis of the a-C:H and a-C:H(N) films adhesion deposited on the substrate, obtained by VDI 3198 indentation test.

Samples	Indentation	Image by ImageJ	Classification	Delaminated Area (%)
DLC			HF2	10.51
DLC(N) 10% N <sub>2</sub>			HF1	5.92
DLC(N) 20% N <sub>2</sub>			HF2	6.89
DLC(N) 30% N <sub>2</sub>			HF1	4.49
DLC(N) 40% N <sub>2</sub>			HF3	11.69
DLC(N) 50% N <sub>2</sub>			HF1	8.25

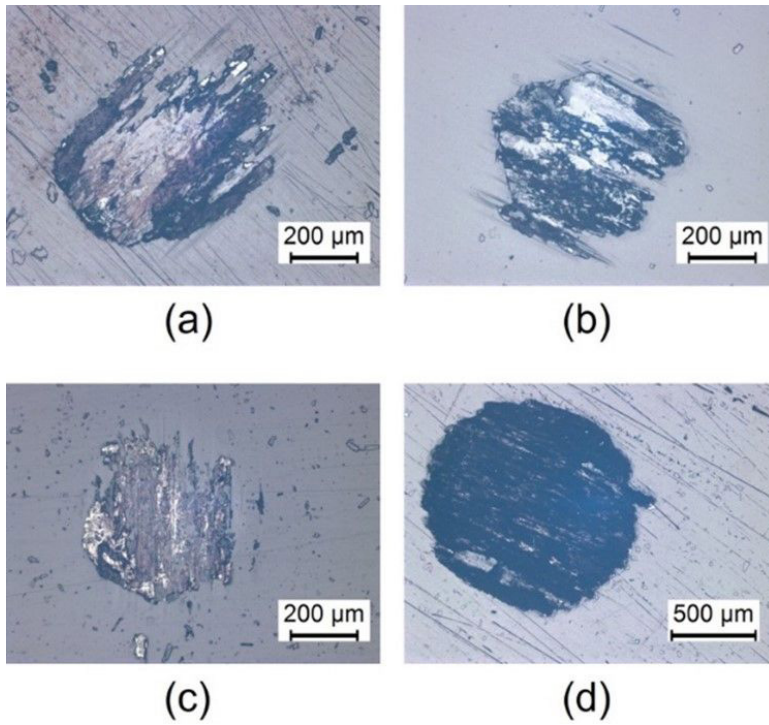
samples exhibiting passive behavior (DLC, DLC(N) 10% N<sub>2</sub>, DLC(N) 20% N<sub>2</sub> and DLC(N) 30% N<sub>2</sub>), a significant drop of  $i_{corr}$  was verified when compared to the uncoated sample, indicating an important enhancement in the corrosion resistance. However, even the samples exhibiting active response (DLC(N) 40% N<sub>2</sub> and DLC(N) 50% N<sub>2</sub>) showed  $i_{corr}$  smaller than the uncoated AISI 321H. Considering the data displayed in this Table the following corrosion resistance ranking can be proposed at the corrosion potential: DLC(N)

30% N<sub>2</sub> > DLC > DLC(N) 10% N<sub>2</sub> > DLC(N) 20% N<sub>2</sub> > DLC(N) 40% N<sub>2</sub>  $\cong$  DLC(N) 50% N<sub>2</sub> > AISI 321H.

Analyzing the responses of the samples presenting passive behavior, in accordance with its lower  $i_{corr}$ , DLC(N) 30% N<sub>2</sub> presented the smallest passive current density, followed by DLC, DLC(N) 10% N<sub>2</sub> and DLC(N) 20% N<sub>2</sub>; moreover, all of them showed a decrease of about two orders of magnitude or more in the passive current density when compared to the uncoated sample, indicating that these coatings

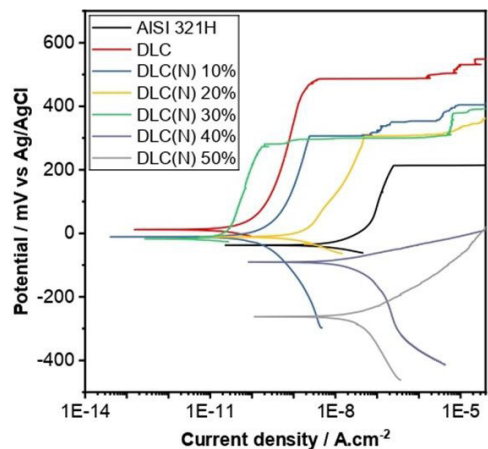
**Table 3.** Electrochemical parameters extracted from the potentiodynamic polarization curves (Figure 6) and impedance modulus ( $|Z| \Omega \cdot \text{cm}^2$ ) at 10 mHz for the samples without and with DLC and DLC(N) films.

Condition	$E_{corr}$ mV vs Ag/AgCl	$i_{corr}$ A.cm <sup>-2</sup>	$E_{pit}$ mV vs Ag/AgCl	$ Z $ at 10 mHz $\Omega \cdot \text{cm}^2$
AISI 321 H	-37.6	$4.71 \times 10^{-8}$	213.0	$1.29 \times 10^5$
DLC	11.5	$9.67 \times 10^{-11}$	486.0	$1.82 \times 10^7$
DLC(N) 10%	-11.0	$3.35 \times 10^{-10}$	306.4	$1.16 \times 10^7$
DLC(N) 20%	-11.64	$2.08 \times 10^{-9}$	303.3	$1.63 \times 10^7$
DLC(N) 30%	-17.5	$2.33 \times 10^{-11}$	294.7	$2.41 \times 10^7$
DLC(N) 40%	-90.8	$7.39 \times 10^{-9}$	-	$9.88 \times 10^5$
DLC(N) 50%	-262.5	$8.18 \times 10^{-9}$	-	$3.91 \times 10^5$


**Figure 5.** Images of the hubcaps obtained in the wear test (a) DLC, (b) DLC(N) 10% N<sub>2</sub>, (c) DLC(N) 30% N<sub>2</sub>, and (d) DLC(N) 50% N<sub>2</sub>.

improve the resistance of the passive layer. Concerning the pitting corrosion resistance, the best response was obtained for the DLC sample, which exhibited the highest pitting potential (+486 mV vs. Ag/AgCl), whereas the N-treated samples showed similar  $E_{pit}$  (306.4 mV vs. Ag/AgCl for the DLC(N) 10% N<sub>2</sub> sample, 303.3 mV vs. Ag/AgCl for the DLC(N) 20% N<sub>2</sub> sample and 294.7 mV vs. Ag/AgCl for the DLC(N) 30% N<sub>2</sub>, which, nevertheless, were about 100 mV more positive than that associated to the uncoated AISI 321H. This indicates that, even though improving the response in relation to the uncoated sample, the presence of N in the DLC films diminishes the resistance to stable pits nucleation and growth.

As discussed before, the DLC and DLC(N) films presented defects produced due to the precipitates present in the substrate or gases blow hole causing the lack of film<sup>11,19</sup>. These defects can influence the corrosion behavior of the material, but the results did not show a correlation with the


**Figure 6.** Potentiodynamic polarization curves of the studied material without and with the DLC and DLC(N) coatings.

percentage of defects of the films with the corrosion behavior of the studied material, once the film that presented lower percentage of defects (DLC(N) 10% N<sub>2</sub>) did not presented the best corrosion behavior, and the film that presented the best corrosion behavior (DLC(N) 30% N<sub>2</sub>) presented an intermediated percentage of defects compared to the studied films.

The analysis of representative corrosion region is showed in Figure 7. It can be observed that the predominant mechanism of corrosion is by the pitting formation (Figure 7a), that induces the dissolution of metal substrate that can promote the unleash of the film from the surface (Figure 7b), as discussed by Campos et al.<sup>11</sup>. Also, the TiN precipitates with rectangular shape, as detached in Figure 7c, presented in this kind of metal can support the corrosion process<sup>40</sup>.

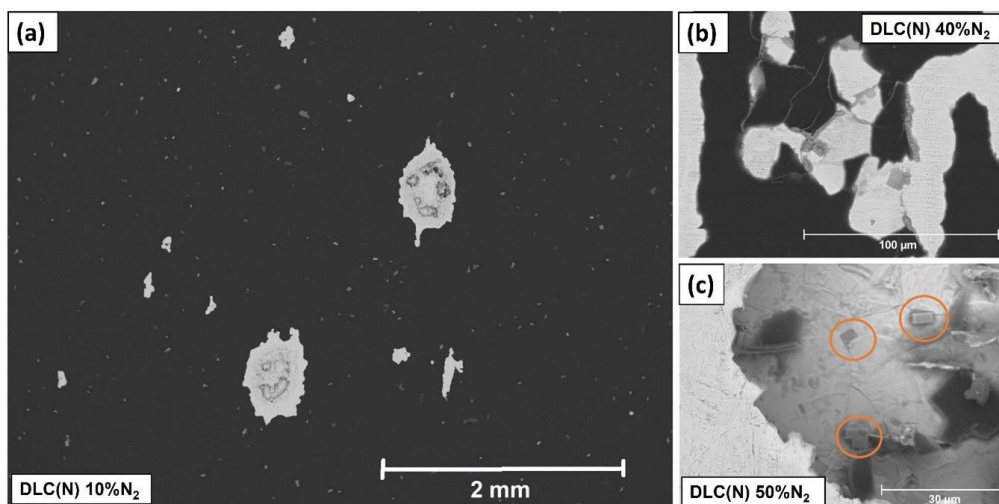
### 3.2.2. EIS behavior

Figure 8 shows the EIS results for the uncoated AISI 321H, DLC and DLC(N) coated samples. In Figure 8a is possible to verify that all the coated samples presented higher impedance modulus values than the uncoated AISI 321H substrate. This outcome is well in agreement with the results of the polarization curves showing that, at the corrosion potential, condition at which the EIS experiments were performed, all the treated samples presented lower  $i_{corr}$  than the uncoated sample. In the phase angle diagrams (Figure 8b), the presence of the different coatings can be ascertained by the capacitive response in the high frequency domain, absent for the uncoated sample. However, this high frequency response was complex and variable for the different samples; therefore, proposing a physical model to interpret these results seems premature and out of the scope of the present investigation. Taking the low frequency (LF) impedance modulus at 10 mHz as a gauge to evaluate the corrosion resistance of the different samples at the corrosion potential (last column in Table 3), it can be verified that, apart from a change of position between samples DLC(N) 10% N<sub>2</sub> and DLC(N) 20% N<sub>2</sub>, it follows quite the same sequence as determined from the polarization curves, showing a good

agreement between the two electrochemical techniques. However, it must be emphasized that the development of localized corrosion in DLC(N) 40% N<sub>2</sub> and DLC(N) 50% N<sub>2</sub> must take place, showing that these two treatments are not adequate concerning corrosion protection, as active sites must be presented even at the corrosion potential.

The corrosion resistance of the coated samples presented in the last paragraphs correlates quite well with the physical properties reported in this investigation. It is shown that the lower the delamination (Figure 3) and the higher the wear resistance (insert of Figure 4) the better the corrosion resistance of the DLC(N) sample, which can be intrinsically correlated with the adhesion of the coatings to the substrate, enhanced by the introduction of N in the coating composition<sup>19,37</sup>. On the other hand, the correlation between the DLC(N) coatings thicknesses and their corrosion resistance seems to be a little bit more intricaded. Initially, it can be considered that increasing the amount of N in the treatment chamber lower the pitting corrosion resistance, as demonstrated by the good correlation between the pitting potential of the coated samples and the amount of N. Therefore, even the DLC(N) 30% N<sub>2</sub> sample, which showed the highest impedance modulus at the corrosion potential, the lowest  $i_{corr}$  and the lowest  $i_{pas}$ , presented a lower pitting potential when compared to the DLC, the DLC(N) 10% N<sub>2</sub> and DLC(N) 20% N<sub>2</sub> samples, even though, as previously stressed, still exhibiting better resistance to localized corrosion than the uncoated substrate. On the other hand, considering the behavior at the corrosion potential, it can be hypothesized that while the N<sub>2</sub> supply does not induce a lowering in the C deposition rate, hindering the film growth process, which seems to occur for N<sub>2</sub> amounts lower than 30%, there is an increase in the overall corrosion resistance of the sample with no significant variation of the coating thickness. However, when more than 40% of N<sub>2</sub> is introduced in the gas composition, the coating thickness decreases leading to a dramatic decrease in its corrosion resistance.

Further, considering the correlation between chemical bonds and structural disorder revealed by the Raman experiments and the corrosion resistance of the DLC(N) coatings, the results



**Figure 7.** Images of the pit obtained in the corrosion test (a) DLC(N) 10% N<sub>2</sub>, (b) DLC(N) 40% N<sub>2</sub>, and (c) DLC(N) 50% N<sub>2</sub>.

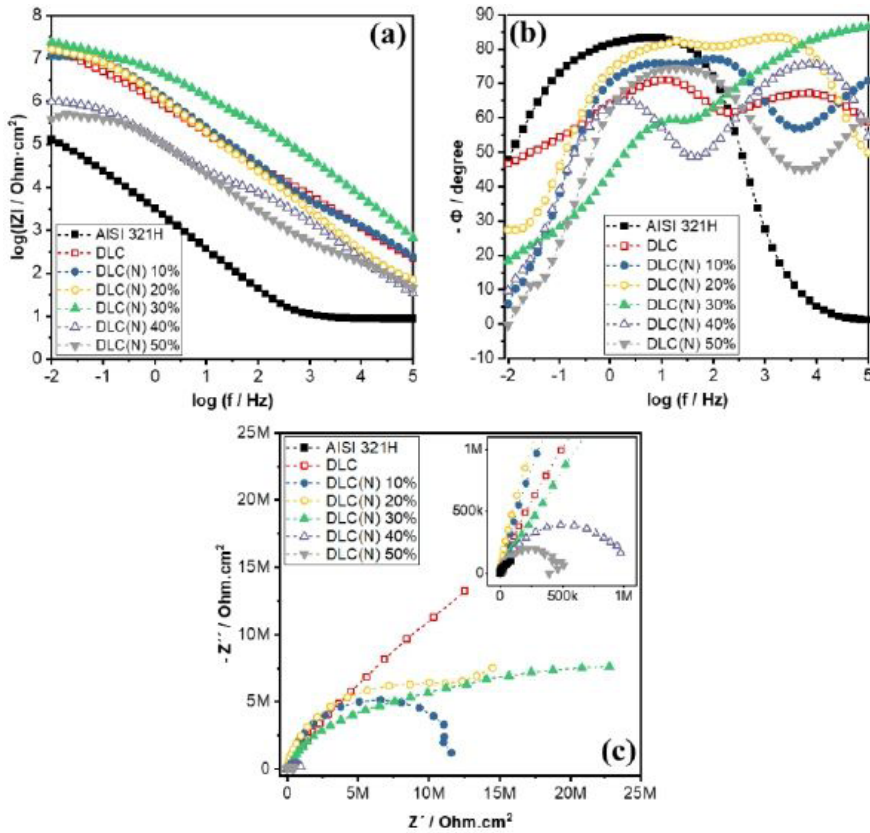


Figure 8. Bode (a,b) and Nyquist (c) diagrams of the different materials.

displayed in Figure 1b and c together with the outcomes of the corrosion tests indicate that there is a saturation limit for the benefic role of N in this property. From these results it is inferred that increasing the graphitic network (higher  $I_D/I_G$  - Figure 1b and decreasing the structural disorder (lower FWHM- Figure 1c) gradually improves the corrosion resistance of the DLC coatings, resulting in higher impedance and lower  $i_{corr}$  and  $i_{pas}$ ; however, at the expenses of localized corrosion resistance, as demonstrated by the lower pitting potential with increasing N content. After the saturation limit of both properties, which seems to be achieved for the DLC(N) 30%  $N_2$  sample, further introduction of N dramatically decreases the localized and the overall corrosion resistance of the samples, which is likely associated with the decrease in the thickness of the protective coating.

Therefore, regarding the corrosion behavior of the DLC(N) coatings, our results indicate that an increase in corrosion resistance can be achieved under optimal conditions, in which increasing  $N_2$  content causes a decrease in the percentage of C-N  $sp^3$  bonds<sup>19</sup>; without, however, the growth of the coating being hampered. As suggested in Figure 1, the DLC(N) 30%  $N_2$  presents a lower percentage of  $sp^3$  C-N bonds<sup>19</sup>, and lower structural disorder (Figure 1c), besides the thickness of the formed layer (about 1.7  $\mu m$ ) is similar to that presented by the DLC coating.

On the other hand, the DLC(N) 40%  $N_2$ , and DLC(N) 50%  $N_2$  conditions showed the worst performance on electrochemical tests, consistent with the high  $I_D/I_G$  ratio

(Figure 1) and lower adhesion property of these films to the substrate. Considering the results reported by Almeida et al.<sup>19</sup>, these films presented a higher percentage of  $sp^3$  C-N bonds, corroborating with the suggestion that this kind of structure presents an important influence in corrosion, adhesion, and wear behavior of the DLC(N) films. Also, the DLC films have defects that allow the corrosive solution to reach the surface of the base material, initiating localized corrosion<sup>11,41</sup>. In the case of the treated stainless steel, the defect can allow the formation of micro-galvanic cells, which can be the driving force for the onset of localized corrosion impairing the corrosion resistance compared with the untreated material, mainly when the defect is produced in a location with the presence of inclusion in the substrates<sup>11</sup>.

#### 4. Conclusions

It is possible to conclude that the DLC films with and without nitrogen incorporation increased the wear resistance of 321H stainless steel. The addition of nitrogen directly influences the properties of DLC films. The nitrogen-free film improved the wear and corrosion resistance of 321H steel. However, the addition of 30%  $N_2$  supply during deposition increased the adhesion, wear, and the corrosion behavior at the corrosion potential of the DLC film to optimal values, while using 40%, and 50% of  $N_2$  impairs the corrosion resistance compared to the base material and DLC film. This result is attributed to a combination of factors such as film structure,

adhesion property, and presence of defective sites in the layer, which reach optimal combination of values at the 30% N<sub>2</sub> concentration. These results are explained by factors such as sp<sup>3</sup> C-C reduction suggested by I<sub>D</sub>/I<sub>G</sub> and FWHM(G) analysis, adhesion properties, and thickness of the formed film. With the results obtained, it is possible to suggest the use of these films in applications where good corrosion and wear resistance properties are required, considering that the incorporation of 30% N<sub>2</sub> favored the improvement of both properties.

## 5. Acknowledgments

The authors would like to thank the University of São Paulo (USP), CEETEPS and UNICAMP. CGS acknowledges the financial assistance of the National Council of Research, Innovation and Technology (CNPq, Brasília-DF, Brazil) under grant 307627/2021-7.

## 6. References

- Silva ES. Efeitos do tratamento térmico de solubilização sobre o crescimento de grão e o grau de sensitização dos aços inoxidáveis austeníticos AISI 321 e AISI 347. São Luís: Universidade Federal do Maranhão; 2007.
- Gobbo C, Pavani RR, Rossino LS, Manfrinato MD. Estudo de corrosão por PIT do aço inox 321H soldado pelo processo GTAW autógeno. São Paulo: FATEC-SP; 2017. Boletim Técnico da FATEC-SP.
- Leban MB, Tisu R. The effect of TiN inclusions and deformation-induced martensite on the corrosion properties of AISI 321 stainless steel. *Eng Fail Anal.* 2013;33:430-8.
- Inagaki M. New carbons: control of structure and functions. Oxford, UK: Elsevier; 2000.
- Grill A. Diamond-like carbon: state of the art. *Diam Relat Mater.* 1999;8(2-5):428-34.
- Dai M, Zhou K, Yuan Z, Ding Q, Fu Z. The cutting performance of diamond and DLC-coated cutting tools. *Diam Relat Mater.* 2000;9(9-10):1753-7.
- Cemin F, Bim LT, Menezes CM, Maia da Costa MEH, Baumvol IJR, Alvarez F, et al. The influence of different silicon adhesion interlayers on the tribological behavior of DLC thin films deposited on steel by EC-PECVD. *Surf Coat Tech.* 2015;283:115-21.
- Neubauer F, Merklein M. Tribological and thermal investigation of modified hot stamping tools. *Tribol Ind.* 2019 Mar 15;41(1):76-89.
- Robertson J. Diamond-like amorphous carbon. *Mater Sci Eng Rep.* 2002;37(4-6):129-281.
- Donnet C, Erdemir A. Tribology of diamond-like carbon films: fundamentals and applications. New York: Springer International Publishing; 2006.
- Campos LAP, Almeida LS, Silva BP, Danelon MR, Aoki IV, Manfrinato MD, et al. Evaluation of nitriding, nitrocarburizing, organosilicon interlayer, diamond-like carbon film and duplex plasma treatment in the wear and corrosion resistance of AISI 4340 steel. *J Mater Eng Perform.* 29(12):8107-21.
- Sharifahmadian O, Mahboubi F, Yazdani S. Comparison between corrosion behaviour of DLC and N-DLC coatings deposited by DC-pulsed PACVD technique. *Diam Relat Mater.* 2019;95:60-70.
- Imai T, Harigai T, Tanimoto T, Isono R, Iijima Y, Suda Y, et al. Hydrogen-free fluorinated DLC films with high hardness prepared by using T-shape filtered arc deposition system. *Vacuum.* 2019;167:536-41.
- Wu W-J, Hon M-H. Thermal stability of diamond-like carbon films with added silicon. *Surf Coat Tech.* 1999;111(2-3):134-40.
- Barros RCM, Ribeiro MC, An-Sumodjo PT, Julião MSS, Serrano SHP, Ferreira NG. Filmes de diamante CVD dopado com boro. Parte I. Histórico, produção e caracterização. *Quim Nova.* 2005;28(2):317-25.
- Franceschini DF, Freire FL, Silva SRP. Influence of precursor gases on the structure of plasma deposited amorphous hydrogenated carbon-nitrogen films. *Appl Phys Lett.* 1996;68(19):2645-7.
- Son MJ, Zhang TF, Jo YJ, Kim KH. Enhanced electrochemical properties of the DLC films with an arc interlayer, nitrogen doping and annealing. *Surf Coat Tech.* 2017;329:77-85.
- Kolawole FO, Tschiptschin AP, Kolawole SK, Ramirez MA. Failure of diamond-like carbon (dlc) coatings in automobile engines – a review. *Proc Eng Sci.* 2019;1(1):171-80.
- Almeida LS, Souza ARM, Costa LH, Rangel EC, Manfrinato MD, Rossino LS. Effect of nitrogen in the properties of diamond-like carbon (DLC) coating on Ti 6 Al 4 V substrate. *Mater Res Express.* 2020;7:1-19.
- Liu C, Hu D, Xu J, Yang D, Qi M. In vitro electrochemical corrosion behavior of functionally graded diamond-like carbon coatings on biomedical Nitinol alloy. *Thin Solid Films.* 2006;496(2):457-62.
- Almeida LS, Moreno de Souza AR, Manfrinato MD, Rossino LS. Estudo do efeito dos parâmetros do tratamento da limpeza a plasma na adesão e resistência ao desgaste de filmes DLC em liga de Ti6Al4V. *Rev Bras Apl Vácuo.* 2020;39:42-55.
- Khun NW, Liu E, Zeng XT. Corrosion behavior of nitrogen doped diamond-like carbon thin films in NaCl solutions. *Corros Sci.* 2009;51(9):2158-64.
- Han BB, Ju DY, Chai MR, Zhao HJ, Sato S. Corrosion resistance of DLC film-coated SUS316L steel prepared by ion beam enhanced deposition. *Adv Mater Sci Eng.* 2019;2019:1-13.
- Cruz D, Souza BA, Campos LAP, Almeida LS, Moreto JA, Manfrinato MD, et al. Projeto, construção e comissionamento de um reator para tratamento de nitretação iônica a plasma em aço P20. *Rev Bras Apl Vac.* 2018;37:102-13.
- Franceschini D, Achete C, Freire F Jr, Mariotto G. Internal stress in nitrogen doped diamond-like a-C:H films. *Mater Res Soc.* 1992;270:481-6.
- Cozza RC, Tanaka DK, Souza RM. Friction coefficient and abrasive wear modes in ball-cratering tests conducted at constant normal force and constant pressure: preliminary results. *Wear.* 2009;267(1-4):61-70.
- Cozza RC. A study on friction coefficient and wear coefficient of coated systems submitted to micro-scale abrasion tests. *Surf Coat Tech.* 2013;215:224-33.
- Rutherford KL, Hutchings IM. A micro-abrasive wear test, with particular application to coated systems. *Surf Coat Tech.* 1996;79(1-3):231-9.
- Sohbatzadeh F, Safari R, Etaati GR, Asadi E, Mirzanejhadi S, Hosseinnejad MT, et al. Characterization of diamond-like carbon thin film synthesized by RF atmospheric pressure plasma Ar/CH<sub>4</sub> jet. *Superlattices Microstruct.* 2016;89:231-41.
- Kasiorowski T, Lin J, Soares P, Lepienski CM, Neitzke CA, de Souza GB, et al. Microstructural and tribological characterization of DLC coatings deposited by plasma enhanced techniques on steel substrates. *Surf Coat Tech.* 2020;389:125615.
- Marciano FR, Almeida EC, Lima-Oliveira DA, Corat EJ, Trava-Airoldi VJ. Crystalline diamond particles into diamond-like carbon films: the influence of the particle sizes on the electrochemical corrosion resistance. *Surf Coat Tech.* 2010;204(16-17):2600-4.
- Casiraghi C, Ferrari AC, Robertson J. Raman spectroscopy of hydrogenated amorphous carbons. *Phys Rev B Condens Matter Mater Phys.* 2005;72(8):085401.
- Vidakis N, Antoniadis A, Bilalis N. The VDI 3198 indentation test evaluation of a reliable qualitative control for layered compounds. *J Mater Process Technol.* 2003;143–144:481-5.
- Heinke W, Leyland A, Matthews A, Berg G, Friedrich C, Broszeit E. Evaluation of PVD nitride coatings, using impact, scratch and Rockwell-C adhesion tests. *Thin Solid Films.* 1995;270(1-2):431-8.

35. Ferrari AC, Robertson J. Resonant Raman spectroscopy of disordered, amorphous, and diamondlike carbon. *Phys Rev B Condens Matter Mater Phys.* 2001;64(7):1-13.
36. Rodil SE, Muhl S. Bonding in amorphous carbon nitride. *Diam Relat Mater.* 2004;13(4-8):1521-31.
37. Leal G, Fraga MA, Rasia LA, Massi M. Impact of high N<sub>2</sub> flow ratio on the chemical and morphological characteristics of sputtered N-DLC films. *Surf Interface Anal.* 2017;49(2):99-106.
38. Cozza RC, Wilcken JT SL, Schön CG. Influence of abrasive wear modes on the coefficient of friction of thin films. *Tecnol em Metal Mater e Mineração.* 2018;15(4):504-9.
39. Trezona RI, Allsopp DN, Hutchings IM. Transitions between two-body and three-body abrasive wear: influence of test conditions in the microscale abrasive wear test. *Wear.* 1999;225–229(I):205-14.
40. Manfrinato MD, de Almeida LS, Rossino LS, Kliauga AM, Melo-Máximo L, Melo-Máximo DV, et al. Scratch testing of plasma nitrided and nitrocarburized AISI 321 steel: influence of the treatment temperature. *Mater Lett.* 2022;317:132083.
41. Ilic E, Pardo A, Suter T, Mischler S, Schmutz P, Hauert R. A methodology for characterizing the electrochemical stability of DLC coated interlayers and interfaces. *Surf Coat Tech.* 2019;375:402-13.